

Three-dimensional kinematic analysis of the golf swing using instantaneous screw axis theory, Part 2: golf swing kinematic sequence

Alessandro Vena · Dave Budney · Tom Forest · Jason P. Carey

Published online: 12 January 2011
© International Sports Engineering Association 2011

Abstract Recent studies have measured body segment rotation to study the kinematic sequence of the downswing. However, this sequence has yet to be determined relative to an instantaneous screw axis (ISA), free to change position and orientation during motion to reflect shifts in a segment's dominant axis of rotation. In Part 2 of this two-part study, the objectives were to compute the amplitude of segment angular velocity relative to the corresponding ISA of that segment and verify if the magnitude of segment angular velocity followed the proximal to distal sequence of the summation of speeds principle. Results indicate that the kinematic sequence of 2 of the 5 subjects analyzed supports the summation of speeds principle, where the sequence in which the maximum angular velocity about the pelvis, shoulders and left arm occurred, for one subject, at 68.2 ± 3.2 , 72.8 ± 1.7 and $100 \pm 0.0\%$ of the downswing.

Keywords Golf · Biomechanics · Kinematics · Instantaneous screw axis

1 Introduction

An important theme in golf swing instruction is the sequence in which the motions that comprise the downswing occur, commonly referred to as the timing of the swing. Proper timing can ensure that club head velocity increases throughout the downswing and achieves a maximum at impact [1, 2]. When discussing the movement of linked segments, the summation of speeds principle [3]

states that motion should follow a proximal to distal sequence. In order to produce the fastest velocity of the most distal segment of the kinematic chain, the motion of large proximal segments must be followed by the faster motion of the smaller distal segments [3]. Cochran and Stobbs [4] were the first to discuss and illustrate through a simple mechanical system, the proximal to distal sequence in the golf swing. Their system consisted of three progressively smaller discs, with coincident centroidal axes, connected with springs. To maximize the velocity of the smallest (distal) disc, each spring should be released when the previous spring has imparted its energy to the system, starting with the largest (proximal) disc. This mechanical analogy can be easily applied to the motion of the lower body, upper body and golf club during the downswing. Many authors have measured the extent and sequence of pelvis, torso and left arm rotation during the golf swing, providing insight into the sequence of the downswing and attempting to establish the relation between body rotation and club head velocity [1, 2, 6–8]. McTeigue et al. [5] and Burden et al. [1] measured spine and hip rotation of professional and amateur golfers and showed that the swing of professional golfers conforms to the summation of speed principle. Robinson [6] studied the correlation between swing characteristics and club head velocity for professional and amateur golfers, identifying angular velocity between the left arm and the shoulders, at impact, and the angular velocity of the hips at the midpoint of the downswing as critical variables. McLaughlin and Best [7] and Myers et al. [8] determined that the rotation angle of the hips and the differential angle between the torso and hips were the statistically significant variables between golfers of various skill levels. Cheetham et al. [2] studied the kinematic sequence of the golf swing, by determining segment angular velocity expressed relative to a segment

A. Vena · D. Budney · T. Forest · J. P. Carey (✉)
University of Alberta, 4-9 Mechanical Engineering Building,
Edmonton, AB T6G 2G8, Canada
e-mail: jason.carey@ualberta.ca

local coordinate frame; for professional golfers, both the maximum angular velocity of each segment and the order in which these maximum values were achieved followed a proximal to distal sequence, supporting the summation of speed principle.

Previous studies computed segment rotation from either the relative angle between two one-dimensional lines projected along the same plane [1, 6–8], such as a line joining the left and right shoulders joints and the line of play [8], or by assuming that the rotation occurs about a fixed point, in which case a fixed coordinate system is imposed [2, 9]. Although later studies do compute full segment angular velocity, coordinate system location and orientation, chosen intuitively, can affect the expression of that segment's angular velocity. This is especially important if the segment rotation does not occur about a fixed point, for example segments that may rotate about multiple joints such as the pelvis. Therefore, it is of interest to compute segment angular velocity from a non-stationary axis. This would not only provide the best representation of a segment rotation, but it would also allow for this instantaneous axis to change position and orientation during the motion to reflect changes in the segment's dominant axis of rotation. These findings were confirmed in Part I of this study [10].

The current study applied instantaneous screw axis (ISA) theory to quantify the kinematic sequence of the golf swing. The main advantage of ISA theory, when compared to an Euler/Cardan angles convention, is that an instantaneous screw axis can change position and orientation during the motion, which cannot be done with the Euler/Cardan angle convention. This is important for such body segments connected to multiple degree of freedom joints, such as the knee or shoulder, which experience rotation and translation. A specific example to golf would be that the rotation of the pelvis should occur about the right leg during the back swing and then about the left leg at impact for a right-handed golfer; use of instantaneous screw axis would show this change in the rotation axis. The methodology of applying ISA theory to the study of the golf swing has been treated in Part 1 [10] of this two-part study.

Objectives of this study were to achieve a better understanding of the rotational components of the golf swing by identifying the location and orientation of the

ISA of the major body segments involved in the golf swing; computing the amplitude of the segment angular velocity, ω , relative to the corresponding ISA of that segment; and, verifying if the amplitude and sequence of the maximum magnitude of angular velocity, ω_{\max} , of the body segments supports the summation of speeds principle [3].

2 Methods

2.1 Subjects

The sampling population consisted of five male, low-handicap, right-handed golfers. The age, physical attributes and golf experience of each subject are summarised in Table 1. Written informed consent was received from all subjects of the study in accordance with the Health Research Ethics Board-Panel B (HREB File # B-131004) requirements.

2.2 Data collection

The displacement of anatomical features was determined from optical motion capture. Data collection was carried out at the Syncrude Centre for Motion and Balance, Glenrose Rehabilitation Hospital, Edmonton, AB, Canada using a Motion Analysis HiRes (Motion Analysis, Santa Rosa, CA, USA) passive-marker optical system. A total of eight cameras (Eagle Digital; Motion Analysis, Santa Rosa, CA, USA) were positioned within the laboratory (Fig. 1) to reduce the occurrence of marker occlusion during the downswing. Data were collected at 400 Hz, as this represents the highest sampling rate at which the cameras could operate at full field of view, to capture the high frequency content of club head motion, without sacrificing measurement accuracy [11]. EVaRT v.4.2 software (Motion Analysis, Santa Rosa, CA, USA) was used to compute marker position, and system calibration was conducted as per manufacturer's procedures. System accuracy was assessed earlier [11]; it was found that the measurement bias and precision were both less than 0.5 mm within the centre of the measurement volume.

Table 1 Sampling population—age, physical attributes and golfing experience of Subjects 1–5

| Subject | Age (years) | Height (m) | Mass (kg) | Experience (years) | Rounds/Year (rounds/year) | Handicap |
|---------|-------------|------------|-----------|--------------------|---------------------------|----------|
| 1 | 26 | 1.78 | 83.9 | 14 | 15 | 6 |
| 2 | 22 | 1.85 | 86.2 | 10 | 20 | 9 |
| 3 | 24 | 1.83 | 81.6 | 11 | 35 | 7 |
| 4 | 40 | 1.85 | 79.4 | 20 | 25 | 10 |
| 5 | 66 | 1.68 | 72.6 | 40 | 25 | 11 |

Reflective markers were placed on the subject's body according to the marker placement guide listed in Table 2 and shown in Fig. 2 as described in Part 1 [10]. Briefly, anatomical landmarks were chosen as the most prominent landmarks of each segment, to limit soft tissue artifact [12] and easily identifiable through manual palpations. In the case of markers being placed on upper limbs, but not at their joints, wrappings were used to reduce the soft tissue artifact. Once the subjects were placed in the capture volume, feet placed in the centre of the volume (as shown in Fig. 1), they were instructed to make smooth, controlled golf swings, consistent with their regular motion aiming to a net on the wall of the room in front of them. Each golf swing was recorded for 10 s duration and a total of five golf swings were analyzed for each subject.

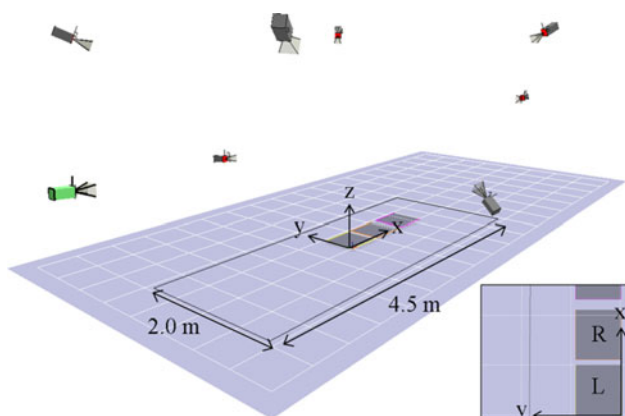


Fig. 1 Optical motion capture system, Syncrude Centre for Motion and Balance. Measurement dimensions are 4.5 m in length (along x -axis), 2.0 m in width (along y -axis) and 2.5 m in height (along z -axis). Right platform (R) and left platform (L) denote foot placement for the stance of subject, with the line of play in the negative x -axis direction. Figure taken from Part 1 [10]

Table 2 Marker placement guide (anatomical landmarks from Moore and Dalley [13])

| Segment | Number of marker | Marker placement | Marker label |
|-----------|------------------|--|--------------|
| Pelvis | 4 | Left anterior superior iliac crest | P_1 |
| | | Right anterior superior iliac crest | P_2 |
| | | Left anterior posterior iliac crest | P_3 |
| | | Right anterior posterior iliac crest | P_4 |
| Shoulders | 4 | Jugular notch | S_1 |
| | | Right acromion | S_2 |
| | | Left acromion | S_3 |
| | | C7 cervical vertebra | S_4 |
| Left arm | 5 | Left elbow, humerus lateral epicondyle | A_1 |
| | | Left elbow, humerus medial epicondyle | A_2 |
| | | Left wrist, radius styloid process | A_3 |
| | | Left wrist, ulna styloid process | A_4 |
| | | Left forearm | A_5 |

2.3 Data analysis

2.3.1 Rigid-body displacement, ISA computation and time normalization

Rigid-body displacement consistent with the measured segment motion was first computed by applying a fourth order low-pass Butterworth digital filter [14] to the measured marker displacements, to attenuate high-order random and systematic instrument noise [15], followed by a solidification procedure [16] to eliminate the relative displacement between markers affixed to the same segment, from the instrument noise [15] and soft tissue artifact [12]. Segment ISA was computed by applying the two-dimensional Reuleaux method presented by Eberharter and Ravani [17] for three homologous points of a rigid-body displacement. Analysis was carried out for the duration of the downswing and normalized in terms of percent downswing completed. The beginning of the downswing characterized as the transition between the backswing and downswing arcs formed by the club head, and impact were both determined from the displacement of a marker placed on the side of the golf club head midway between the toe and heel. These methodologies were further discussed in Part 1 [10] and were followed in the current study.

2.3.2 Computed variables

Golf swing kinematic sequence was determined by studying the angular velocity of each segment relative to their ISA. The time at which the maximal magnitude of the angular velocity was determined as the order in which the segments sequentially achieve their respective maximum yields the kinematic sequence. ω_{\max} and the percent downswing were computed at the instant where each ISA achieved its respective maximum angular velocity.

Fig. 2 Marker placement guide; **a** front view, **b** rear view

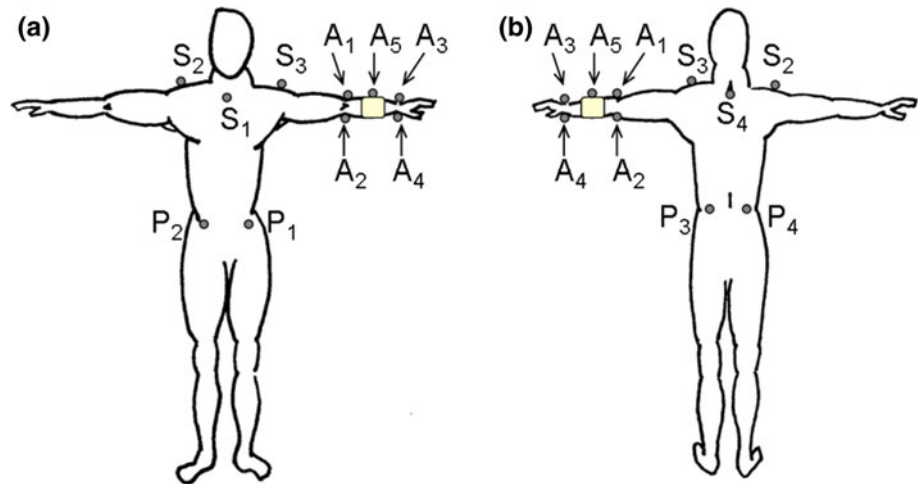
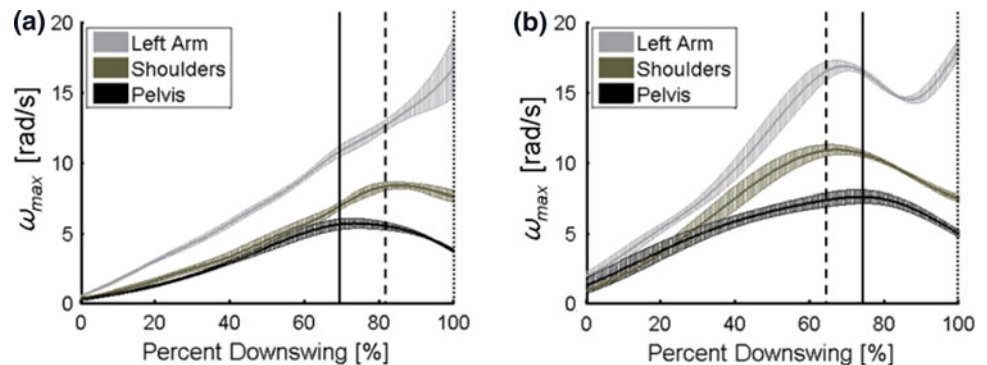


Fig. 3 Magnitude of segment angular velocity about their ISA; **a** Subject 1, **b** Subject 2. Vertical lines coincide with maximum segment ω_{\max} : *solid line* for the pelvis, *dashed line* for the shoulders and *dotted line* for the left arm



3 Results

To illustrate the process of computing segment angular velocity and determining the kinematic sequence, results have been divided into two sections. The first will discuss time varying segment angular velocity, for the duration of the downswing, while the second section will focus on the instant of maximum segment angular velocity.

3.1 Time varying angular velocity

The magnitude of the angular velocity about each ISA was plotted as a function of percent downswing. Each angular velocity, one for each ISA, was plotted as the mean magnitude plus or minus one standard deviation. The results for Subjects 1 and 2 are shown in Fig. 3, each chosen to illustrate a different sequence observed in this study. In the case of Subject 1, the magnitude and percent downswing of segment angular velocity both increase from the most proximal segment (pelvis) to the most distal segment (left arm) of the kinematic chain. This proximal to distal sequence can also be seen with Subjects 3 and 4. In the case of Subject 2, the magnitude of segment velocity increases also from proximal to distal. However, the

percent downswing at which these maximum angular velocities occur does not follow a proximal to distal sequence, as the angular velocity of the shoulders achieves its maxima before the pelvis. This sequence is also shared by Subject 5.

3.2 Magnitude and sequence of maximum segment angular velocity

The kinematic sequence of the downswing was quantified by computing the magnitude of the segment angular velocity when maximized, as well as identifying the percent downswing corresponding to that instant. The maximum angular velocity ω_{\max} about the pelvis (ISA_P), shoulders (ISA_S), and left arm (ISA_A), are shown in Fig. 4 for each subject. The results indicate that, for all subjects, the magnitude of the segment angular velocity increases from the most proximal segment (pelvis) to the most distal segment (left arm). Furthermore, the instant corresponding to these maximum angular velocities is shown in Fig. 5. In the case of Subjects 1, 2 and 3, there are apparent differences between the instances corresponding to each ω_{\max} between segments, indicating the presence of a distinct kinematic sequence. There is overlap of the “time band” in

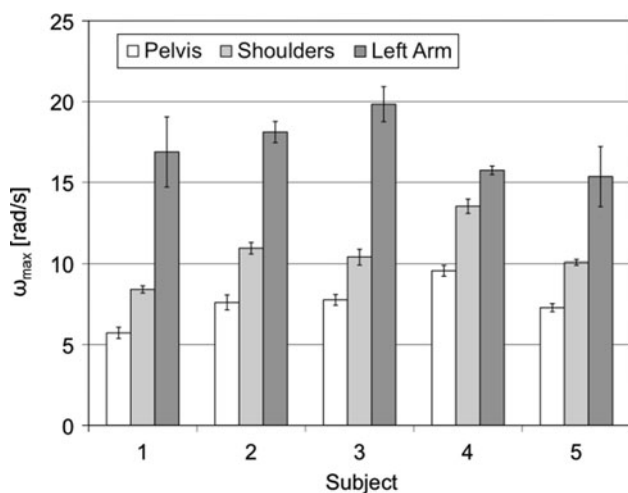


Fig. 4 Subjects 1–5: mean ω_{max} , with standard deviation error bars, about the pelvis, the shoulders and the left arm

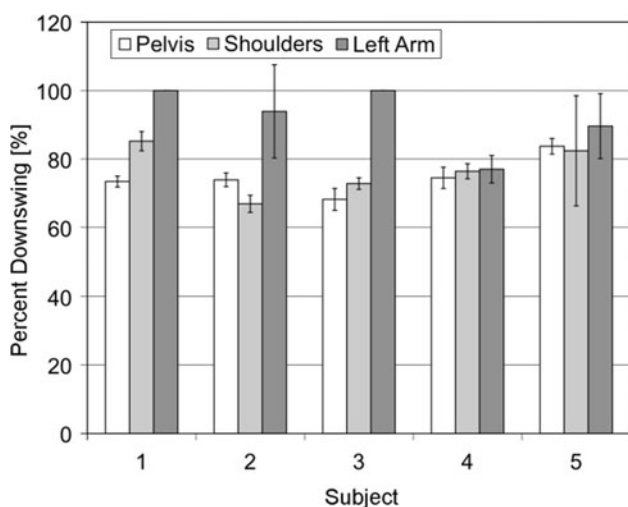


Fig. 5 Subjects 1–5: mean percent downswing corresponding with maximum segment angular velocity about the pelvis, the shoulders and the left arm. Percent downswing is presented with standard deviation error bars

some subjects. There is no overlap for subjects 1, 2 and 3 but all three maxima overlap for Subjects 4 and 5 within a time band of the mean ± 1 standard deviation. For Subjects 1 and 3 the sequence at which each ISA achieves its maximum angular velocities is as follows: pelvis, shoulders and left arm. This sequence shows the progression from the most proximal segment to the most distal segment. For Subject 2, the sequence at which each ISA achieves its ω_{max} is as follows: shoulders, pelvis and left arm. Although the angular velocity about the left arm achieves its maximum last, the angular velocity about the shoulders reached its maximum before the angular velocity about the pelvis. For Subjects 4 and 5, no distinct sequence can be

determined due to the high standard deviations (Subject 5) and the closeness in mean values (Subject 4).

4 Discussion

The kinematic sequence of the golf swing was determined by studying the angular velocity of each segment relative to their ISA. Furthermore, the instant where the magnitude of angular velocity is maximized were thoroughly analyzed, as the order in which segments sequentially achieve their respective maximum yields the kinematic sequence.

4.1 Time varying angular velocity

Angular velocity curve profile, relative magnitude and sequence of maximum angular velocity between the segments were used to compare the angular velocity of the five subjects.

4.1.1 Angular velocity curve profile

For Subjects 1–4, the angular velocities about ISA_P and ISA_S , as a function of percent downswing, appear as near bell curves as seen in Fig. 3 of Subject 1. As for Subject 5, the profile of the angular velocity about ISA_P is also a near bell curve, while the angular velocity about ISA_S increased up to a maximum value and was nearly maintained until impact. The near bell shaped curves were the expected results, as the rotations about the pelvis and shoulders are expected to increase steadily, until attaining a maximum value, and to decrease before impact [18]. As the pelvis and shoulders are proximal segments in the kinematic chain of the golf swing, their angular velocities are expected to slow down before impact and in the process transmit their momentum to the more distal segments. The observed results are in line with the summation of speeds principle [3].

Conversely, the angular velocity about ISA_A displays more variability in profile when comparing all subjects. For Subjects 1 and 5, the angular velocity about ISA_A increases until impact, maintaining a positive slope throughout the downswing. For Subjects 2, 3 and 4 the angular velocity about ISA_A has a near bell shape profile followed by an increase until impact, occurring at approximately 85–90% downswing, as seen in Fig. 3 for Subject 2. This angular velocity profile was also shown by Cheetham et al. [2] for Amateur 1, although the increase occurred after impact. The motion of the left arm can be thought to have two components, rotation about the left glenohumeral joint and supination of the left wrist. To satisfy the summation of speeds principle [3], it

is expected that the rotational velocity about the left shoulder would decrease before impact, while wrist supination increases in velocity into impact. It is postulated that the profiles of Subjects 2, 3 and 4 show this distinction: the first portion of the curve, near bell shaped, denotes rotation about only the left shoulder joint while the second portion, which shows increasing velocity up to impact, denotes the added contribution of wrist supination. As the arm was assumed rigid from the shoulder to the wrist, the ISA reflects motion about the shoulder joint as well as about the wrist. Therefore, the ISA represent a “hybrid” axis of rotation for the left arm.

4.1.2 Relative magnitude and sequence of maximum angular velocity

For all subjects, the magnitude of each maximum angular velocity ω_{\max} increases from the most proximal segment (pelvis) to the most distal segment (left arm) as expected as the velocity increases from the contribution of each segment in the kinematic chain. However, the sequence at which the maximum angular velocities occur is not the same for all subjects. The results of Kenny et al. [19] for segmental sequencing of kinetic energy in a computer-simulated golf swing indicate a subjective optimal coordination of sequencing, reinforcing the benefit of single-subject in their analysis of the golf swing. Putnam et al. [18] showed kinematic sequencing. While work on tennis service analysis [20] has shown that for some subjects, angular velocities peak simultaneously. The results of this study show both types of behaviour. For Subjects 1 and 3, the sequence is pelvis, shoulders and left arm, the desired progression following the summation of speed principle [3]. It is consistent with the sequence computed by Cheetham et al. [2] for one professional golfer. For Subject 4, the sequence of mean maximum angular velocities appears to be similar, where proximal segments achieve their maximum before the most distal segment. However, it cannot be said that this follows the desired proximal to distal sequence, as statistically significant differences between these instances could not be found. The results of Subjects 1 and 3 confirm that the start of the downswing coincided with the motion of the pelvis [1, 2, 5]. This is not the case for Subject 2; the sequence at which each ISA achieves its maximum angular velocities is the shoulders, pelvis and left arm. Here the maximum angular velocity about the shoulders is reached before the angular velocity about the pelvis. This sequence appears to be shared by Subject 5, however, high standard deviation in the motion about the shoulders prevents any conclusions to be drawn. Thus, two of five subjects achieved their maximum angular velocities in the desired kinematic sequence.

4.2 Magnitude and sequence of maximum segment angular velocity

The magnitude and percent downswing corresponding to the maximum segment angular velocity were determined for each ISA and the subject are discussed for each corresponding ISA.

4.2.1 Pelvis ISA (ISA_P)

The maximum angular velocity ω_{\max} about ISA_P ranged from 5.72 ± 0.35 rad/s, for Subject 1, to 9.56 ± 0.34 rad/s, for Subject 4. The standard deviation on ω_{\max} ranged from 0.25 rad/s, for Subject 5, to 0.47 rad/s, for Subject 2, which represents 3.4 and 6.6% relative to their corresponding mean ω_{\max} , respectively. This reveals that the magnitude of ω_{\max} is consistent within all subjects, as the standard deviation represents less than 10% of the mean value. This is also within the likely swing performance variation expected from this level of player seen in similar studies [2, 8]. Club head impact velocity shows consistency for each player over all trials; the maximum value of standard deviation as a percentage of the mean is 3.6%. The maximum angular velocities about ISA_P are consistent with the pelvic angular velocity determined by Cheetham et al. [2], who reported values of 6.89 ± 1.19 rad/s for amateurs and 8.33 ± 0.93 rad/s for professionals. Of all subjects, only the angular velocity of Subject 4 was not contained within the one standard deviation of these two means. Furthermore, the computed maximum angular velocities of the pelvis are also consistent with the results from Myers et al. [8], who reported the maximum rate of change of a pelvis angle to be 6.241 ± 1.018 rad/s for low ball speed players and 7.568 ± 1.274 rad/s for high ball speed players. It is important to note that their results do not represent the angular velocity of the pelvis, but an approximation given by the rate of change of the angle between a one-dimensional line along the pelvis, connecting the left and right anterior superior iliac crests, and the line of play.

The instant corresponding to ω_{\max} of each subject varied from $68.2 \pm 3.2\%$ downswing, for Subject 3, to $83.7 \pm 2.3\%$ downswing, for Subject 5. This indicates that for all subjects the maximum angular velocity occurs in the last 1/3 of the downswing. The standard deviation of the corresponding instances ranged from 1.6% downswing (Subject 1) to 3.2% downswing (Subject 3). These percent downswings are slightly above those published by Cheetham al. [2] for professional golfers. Although results were not explicitly given, the instance of maximum pelvis angular velocity was determined from interpolation of the given angular velocity plot, of a professional golfer, and from the given downswing duration. From these

procedures, an approximate percent downswing value of 60% was computed, which was 8.2% lower than the lowest mean value computed in this study. These results indicate that the professional golfer from Cheetham et al. [2] fired his hips earlier in the downswing, perhaps in an attempt to create greater separation between the hips and shoulders, as this has been shown to be one of the swing variables with the highest correlation to club head velocity [7].

4.2.2 Shoulders ISA (ISA_S)

The maximum angular velocity about ISA_S ranged from 8.41 ± 0.22 rad/s (Subject 1) to 13.51 ± 0.44 rad/s (Subject 4). The standard deviation on ω_{\max} ranged from 0.22 rad/s (Subject 1) to 0.47 rad/s (Subject 3), which represents 2.7 and 4.5% relative to their corresponding mean ω_{\max} , respectively, revealing that the magnitude of ω_{\max} is consistent within all subjects, as the standard deviation represents less than 5% of the mean value. The maximum angular velocities about ISA_S are consistent with the thorax angular velocity determined by Cheetham et al. [2], who reported values of 10.18 ± 1.47 rad/s for amateurs and 12.69 ± 1.06 rad/s for professionals. Of all subjects, only the mean angular velocity of Subject 1 was not contained within the one standard deviation of these two means. Furthermore, the computed maximum angular velocities of the shoulders are also consistent with the results from Myers et al. [8], who reported the maximum rate of change of a torso angle to be 10.318 ± 1.166 rad/s for low ball speed players and 13.380 ± 1.274 rad/s for high ball speed players. As was the case for the pelvis, it is important to note that their results represent an approximation given by the rate of change of the relative angle between a one-dimensional line along the shoulders, connecting the left acromion and right acromion, and the line of play.

The instant corresponding to the ω_{\max} of each subject varied from $66.9 \pm 2.5\%$ downswing (Subject 2) to $85.2 \pm 16.1\%$ downswing (Subject 5). This indicates that for all subjects the maximum angular velocity occurs in the last 1/3 of the downswing. The standard deviation of the corresponding instances ranged from 1.7% downswing (Subject 3) to 16.1% downswing (Subject 5). These results approach those published by Cheetham et al. [2] for professional golfers, which were estimated at an approximate percent downswing value of 70%, which is contained within the subject values of this study. The percent downswings of Subjects 2, 3 and 4 were all within 7% of the professional data of Cheetham et al. [2], while Subjects 1 and 5 differed by 15.2 and 12.4%, respectively. Although Subject 1 differed by 15.2%, a difference of 11.8% was maintained between the maximum angular velocities of the pelvis and shoulders, which resembles the percent

difference between the pelvis and shoulders of the professional golfer published by Cheetham et al. [2].

4.2.3 Left Arm ISA (ISA_A)

The maximum angular velocity about ISA_A ranged from 15.44 ± 1.86 rad/s (Subject 5) to 19.83 ± 1.08 rad/s (Subject 3). The standard deviation on ω_{\max} ranged from 0.27 rad/s (Subject 4) to 2.17 rad/s (Subject 1), which represents 1.7 and 12.9% relative to their corresponding mean ω_{\max} , respectively, revealing that the magnitude of ω_{\max} about the left arm is more variable than about the pelvis and shoulders, as the standard deviation for some subjects represents more than 10% of the mean value. The maximum angular velocities about ISA_A were higher in magnitude than the arm angular velocity determined by Cheetham et al. [2], who reported values of 13.32 ± 1.66 rad/s for amateurs and 17.10 ± 1.19 rad/s for professionals. The angular velocity of all subjects exceeded the angular velocity of the amateur group, which was not unanticipated as the subjects of the current study are all of low handicap. However, it was unexpected that the angular velocity of Subjects 2 and 3 exceeded the magnitude of the professionals. Cheetham et al. [2] reported only one component of left arm angular velocity, perpendicular to the instantaneous swing plane defined by the position of the left arm and golf club shaft. Therefore, this may have contributed to the disparities with the angular velocities of the current study. Again, ISA does not differentiate the motion of the arm about the shoulder joint and wrist joint and the hybrid results presented is to be expected.

The instant corresponding to the ω_{\max} of each subject varied from $77.0 \pm 24.0\%$ downswing (Subject 4) to $100.0 \pm 0.0\%$ downswing (Subjects 1 and 3). This indicates that for all subjects the maximum angular velocity occurs in the last 1/3 of the downswing, and for Subjects 1 and 3 the angular velocity continued to increase into impact. The standard deviation of the corresponding instances ranged from 0.0% downswing (Subjects 1 and 3) to 13.6% downswing (Subject 2). Only the results of Subject 4 approach those published by Cheetham et al. [2] for a single professional golfer. From interpolation of the given angular velocity plot, an approximate percent downswing value of 75% was computed, which approaches the value of Subject 4, of 77% downswing. As the angular velocity values published by Cheetham et al. [2] were computed perpendicular to the swing plane, arm motion from wrist supination was not included in the computation. Furthermore, it would appear that the ISA_A of Subject 4 displayed the least amount of similarity with the supination axis as seen in Table 3. Therefore, it is suggested that the angular velocity about ISA_A reflects the

Table 3 Left arm ISA orientation computed relative to the spine axis and the supination axis of the forearm

| Subject | Orientation | | | |
|---------|---------------|-------------|-----------------|-------------|
| | Spine axis | | Supination axis | |
| | Mean (degree) | SD (degree) | Mean (degree) | SD (degree) |
| 1 | 8.86 | 2.42 | 33.71 | 6.85 |
| 2 | 9.38 | 1.44 | 38.47 | 27.49 |
| 3 | 21.83 | 3.59 | 31.14 | 7.03 |
| 4 | 4.51 | 0.79 | 83.56 | 3.09 |
| 5 | 15.71 | 2.26 | 67.17 | 18.49 |

rotation of the left arm about the left glenohumeral joint, which would explain the proximity to the results of Cheetham al. [2], while the angular velocity of Subjects 1 and 3 reflects a combination of shoulder rotation and wrist supination. For these subjects, the deceleration of the left arm prior to impact is less apparent, as the supination of the left wrist occurs into impact. If it is desired to isolate the rotation of the left arm about the shoulder joint, this could be by using markers S_3 , A_1 and A_2 (shown in Fig. 2) during ISA computation, thus analysing the motion of the upper left arm only.

5 Conclusion

The main objective of the current study was to quantify the kinematic sequence of the golf swing by applying ISA theory, thus computing segment rotation relative to a non-stationary gross axis of rotation. Closeness in the magnitude of maximum segment angular velocity has been found by previous investigators, computed from both the rate of the relative angle between two one-dimensional lines projected along the same plane and from the change in orientation of a fixed technical reference frame. Results indicate that the kinematic sequence of 2 of the 5 subjects analyzed supports the summation of speeds principle, as the order in which maximum segment angular velocity occurs follows a proximal to distal sequence. This supports the finding of previous investigators for professional golfers, where the maximum angular velocity about the pelvis, shoulders and left arm have been shown to occur at approximately 60, 70 and 75% downswing, respectively. Subject 3 displayed the highest proximity to this sequence of professional golfers, with corresponding percent downswings of 68.2 ± 3.2 , 72.8 ± 1.7 and $100 \pm 0.0\%$. This represents the first analysis where the proximal to distal sequence has been confirmed for motion about an ISA. Furthermore, this methodology has illustrated the difference in kinematic sequence between subjects, showing its value as an assessment tool for

instruction. This is a very exciting result for the analysis of the golf swing, as the current model not only provides a quantifiable measure of the kinematic sequence, but each maximum can occur about a non-stationary axis, which is free to change position and orientation to reflect shifts in the segment's dominant axis of rotation. Therefore, ISA theory represents an effective tool in the analysis of the golf swing.

References

- Burden AM, Grimshaw PN, Wallace ES (1998) Hip and shoulder rotations during the golf swing of sub-10 handicap players. *J Sports Sci* 16:165–176
- Cheetham PJ, Rose GA, Hinrichs RN, Neal RJ, Mottram RE, Hurriion PD, Vint PF (2008) Comparison of kinematic sequence parameters between amateur and professional golfers. In: Crews D, Lutz R (eds) *Science and golf V: proceedings of the World scientific congress of golf*, Phoenix, United-States
- Bunn JW (1972) *Scientific principles of coaching*. Prentice-Hall, New Jersey
- Cochran A, Stobbs J (1968) *The search for the perfect swing*. JB Lippincott, New York
- McTeigue M, Lamb SR, Mottram R, Pirozzolo F (1994) Spine and hip motion analysis during the golf swing. In: AJ Cochran, MR Farrally (Eds.) *Science and golf II: proceedings of the World scientific congress of golf*, St Andrews, Scotland
- Robinson RL (1994) A study of the correlation between swing characteristics and club head velocity. In: AJ Cochran, MR Farrally (Eds.) *Science and golf II: proceedings of the World scientific congress of golf*, St Andrews, Scotland
- McLaughlin PA, Best RJ (1994) Three-dimensional kinematic analysis of the golf swing. In: AJ Cochran, MR Farrally (Eds.) *Science and golf II: proceedings of the World scientific congress of golf*, St Andrews, Scotland
- Myers J, Lephart S, Tsai Y-S, Sell T, Smoliga J, Jolly J (2008) The role of upper torso and pelvis rotation in driving performance during the golf swing. *J Sports Sci* 26:181–188
- Teu KK, Kim W, Fuss FK, Tan J (2006) The analysis of golf swing as a kinematic chain using dual Euler angle algorithm. *J Biomech* 39:1227–1238
- Vena AS, Budney D, Forest T, Carey JP (2011) Three-dimensional kinematic analysis of the golf swing using instantaneous screw axis theory, Part 1: methodology and verification. *Sports Eng* (in press)
- Vena A, Carey J, Liggins A, Kawchuck G (2008) Effect of sampling rate on accuracy and relative error of motion capture: system evaluation for golf biomechanics research. In: Fahim A (ed) *Canadian society of mechanical engineering forum 2008*. Ottawa, Canada
- Leardini A, Chiari L, Della Croce U, Cappozzo A (2005) Human movement analysis using stereophotogrammetry. Part 3. Soft tissue artifact assessment and compensation. *Gait Posture* 21:212–225
- Moore KL, Dalley F (2006) *Clinically oriented anatomy*, 5th edn. Lippincott Williams & Wilkins, Baltimore
- Winter DA (2004) Kinematics. In: *Biomechanics and motor control of human movement*, 3rd edn. Wiley, NJ, pp 13–58
- Chiari L, Della Croce U, Leardini A, Cappozzo A (2005) Human movement analysis using stereophotogrammetry. Part 2: Instrumental errors. *Gait Posture* 21:197–211

16. Chèze L, Fregly BJ, Dimnet J (1998) Determination of joint functional axes from noisy marker data using the finite helical axis. *Hum Mov Sci* 17:1–15
17. Eberharter JK, Ravani B (2006) Kinematic registration in 3D using the 2D Reuleaux method. *J Mech Des* 128:349–355
18. Putnam CA (1993) Sequential motions of body segments in striking and throwing skills: descriptions and explanations. *J Biomech* 26:125–135
19. Kenny IC, McCloy AJ, Wallace ES, Otto SR (2008) Segmental sequencing of kinetic energy in a computer-simulated golf swing. *Sports Eng* 11:37–45
20. Van Gheluwe B, Hebbelinck M (1985) The kinematics of the service movement in tennis: a three-dimensional cinematographical approach. In: Winter DA, Norman RW, Wells RP, Hayes KC, Patla AE (eds) *Biomechanics IX-B*. Human Kinetics, Champaign